Extended Abstracts of the 2003 International Conference on Solid State Devices and Materials, Tokyo, 2003, pp. 64-65

C-2-5

Enhancement of dielectric constant due to expansion of lattice spacing in CeO_2 directly grown on Si (111)

Daisuke Matsushita, Yukie Nishikawa, Nobutaka Satou*, Masahiko Yoshiki*, Tatsuo Schimizu, Takeshi Yamaguchi, Hideki Satake and Noburu Fukushima

Advanced LSI Technology Laboratory, Toshiba Corporation and *Toshiba Nanoanalysis Corporation
1, Komukai-Toshiba-cho, Saiwai-ku, Kawasaki 212-8582, Japan
Phone:+81-44-549-2192, Fax:+81-44-520-1257, d-matsushita@amc.toshiba.co.jp

1. Introduction

Crystalline oxide is a candidate for gate dielectrics, which can realize equivalent oxide thickness (EOT) less than 0.5 nm. We achieved direct growth of CeO_2 on Si (111) and EOT as thin as 0.38 nm [1]. The dielectric constant (ε) of the CeO_2 was 52, which is twice as large as the reported value of bulk (polycrystalline) CeO_2 (ε~26). The value of ε in ionic oxide is strongly related with crystal structures and/or lattice spacings. Enhancement of ε by changing the crystal structure of Ta_2O_3 was reported [2], but the crystalline symmetry is unchanged in the CeO_2 case. Anisotropy in ε may not be existent in fluorite structures such as CeO_2. The relationship between the lattice spacings and ε theoretically studied in $SrTiO_3$ [3] and we supposed that the changes in lattice spacing in CeO_2 may be a considerable reason. In this study, we preciously evaluated the lattice spacings of CeO_2 directly grown on Si (epitaxial CeO_2) and discussed the ε enhancement characteristics.

2. Sample preparation

CeO_2 was grown on p-Si (111) substrate by molecular beam epitaxy (MBE) using metal Ce and O_3 as source materials at 700 ºC. The thickness of CeO_2 was 10 nm. Fig.1 (a) is a cross-sectional TEM image of the CeO_2/Si (111) interface and (b) is a plane view TEM image of CeO_2. CeO_2 is confirmed to be single crystalline and directly grown on Si without any interfacial layer.

3. Results and discussions

To evaluate lattice spacings in ultra thin films, we performed in-plane XRD measurements [4], whose schematic diagrams are shown in Figs. 2. Reciprocal space maps around (220) planes for (a) Si substrate and (b) CeO_2/Si were measured to separate Si and CeO_2 peaks as shown in Figs. 3. Ellipses in Figs. 3 indicate FWHM of diffraction peaks for Si and CeO_2, which are determined by the peak separation method using gaussian curves. In Fig. 3 (b), a broad diffraction pattern of CeO_2 with a sharp Si diffraction pattern was observed. It can be seen that the 2θ angle of CeO_2 is lower than that of Si. It means that the lattice spacing of CeO_2 (110) ($d_{CeO2(110)}$) is larger than that of Si (110) ($d_{Si(110)}$). The relative change in $d_{CeO2(110)}$ from Si ($\Delta d_{CeO2(110)}$) is calculated to be +0.26 %.

Electron diffraction patterns (EDP) were observed by TEM [5] to examine the lattice spacing parallel to the sample surface ($d_{CeO2(111)}$), in addition to $d_{CeO2(110)}$, as shown in Fig. 4. We can obtain $\Delta d_{CeO2(110)}$ and $\Delta d_{CeO2(111)}$ by comparing the spot positions of CeO_2 with those of Si. Table I summarizes $\Delta d_{CeO2(110)}$ and $\Delta d_{CeO2(111)}$ by in-plane XRD and EDP. The value of $d_{CeO2(111)}$ is also larger than $d_{Si(111)}$ ($\Delta d_{CeO2(111)}$ = +0.3 %). $\Delta d_{CeO2(110)}$ by EDP is evaluated to be +0.3 %, which agrees with the in-plane XRD result. The lattice constant of bulk CeO_2 is reported to be 0.541 nm which is smaller than that of Si (0.543 nm) by –0.35 %. It is found that the lattice spacings in epitaxial CeO_2 are isotopically expanded by 0.6 %, compared with those in bulk CeO_2.

We focused on the lack of oxygen in CeO_2 as a reason for the expansion of the lattice spacings. Because it is reported that Ce oxides have two crystal structures as CeO_2 and Ce_2O_3 and that the lattice constant of Ce_2O_3 is larger than that of CeO_2 by 3 % [6]. As the number of oxygen atoms in a unit cell of Ce_2O_3 is smaller than that of CeO_2, the coulomb interaction in Ce_2O_3 would be lowered compared with that in CeO_2, resulting in expansion of the lattice constant in Ce_2O_3. In order to confirm the lack of oxygen in epitaxial CeO_2, we performed X-ray photoelectron spectroscopy (XPS) measurements. Additional in-gap state is observed in the valence band edge spectrum as shown in Fig. 5, which is determined to be due to the oxygen-defect-induced state [7]. This result indicates that the expansion of lattice spacings in epitaxial CeO_2 is due to the lack of oxygen atoms.

We consider that the enhancement of ε is due to the expansion of the lattice spacings in epitaxial CeO_2 as described above. This tendency is similar to the result of $SrTiO_3$[3] as shown in Fig. 6. However, the enhancement of ε in CeO_2 is smaller than that of $SrTiO_3$. It may indicate that the ε enhancement mechanism in CeO_2 is different from that in $SrTiO_3$; for example, the contribution of ionic polarizations on ε, or the changes of electron states around Ce atoms due to oxygen defects.

4. Conclusions

We found that the lattice spacings in CeO_2 directly grown on Si are expanded compared with those in bulk CeO_2 due to the oxygen defects and that causes ε enhancement in epitaxial CeO_2. This result indicates that we can control the dielectric constant with the quantity of oxygen atoms in ionic crystalline oxides.

References

[1] Y. Nishikawa, N. Fukushima, N. Yasuda, K. Nakayama and S. Ikegawa, Jpn. J. Appl. Phys. 41, (2002) 2480.
[2] M. Hiratani, T. Hamada, S. Iijima, Y. Ohji, I. Asano, N. Nakanishi and S. Kimura, *Dig. Tech. Papers Symp. VLSI Tech., Kyoto*, 2001, p41.
[3] T. Schimizu and T. Kawakubo, Jpn. J. Appl. Phys. 37, (1998) L235.
[4] H. Tomita, S. Komiya, Y. Horii and T. Nakamura, Jpn. J. Appl. Phys. 34, (1997) L876.
[5] M. Koguchi, K. Nakamura and K. Umemura, *Ext. Abst. SSDM 2001, Tokyo*, (2001) p198.
[6] N. V. Skorodumova, R. Ahuja, S. I. Simak, I. A. Abrikosov, B. Johansson and B. I. Lundqvist, Phys. Rev. B 64, (2001) 115108.
[7] A. Pfau and K. D. Schierbaum, Surf. Sci. 321, (1994) 71.

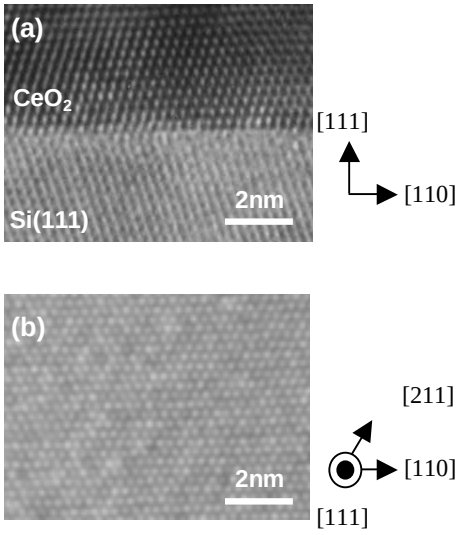

Fig. 1 (a)Cross-sectional view and (b)plane view TEM images of CeO_2/Si(111).

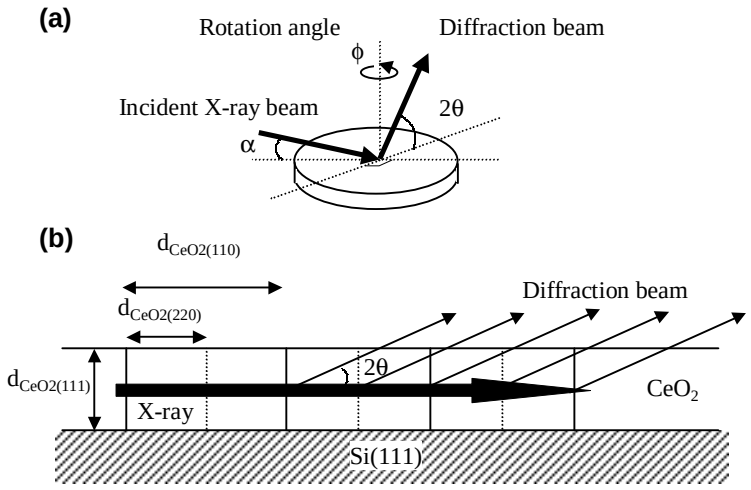

Fig. 2 Schematic diagrams of in-plne X-ray diffraction (XRD) measurements. (a) Geometry for incident and diffraction beams. X-ray is irradiated under critical angle of CeO_2. (b)Direction of X-ray propagation in CeO_2/Si(111). Lattice spacings perpendicular to sample surface can be obtained.

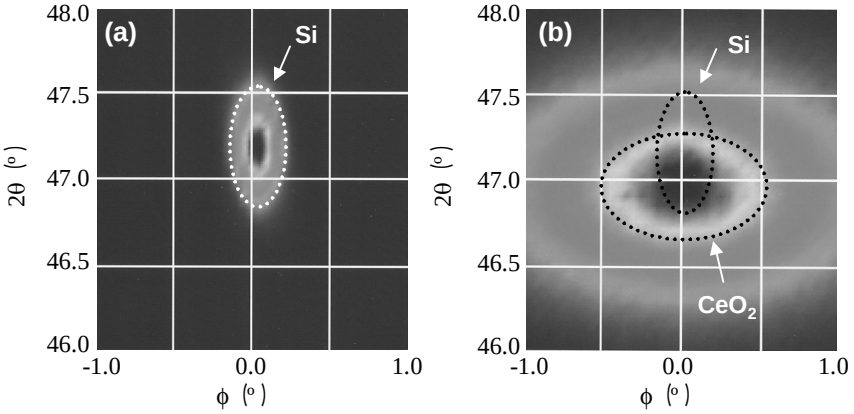

Fig.3 Reciprocal space maps around Si(220) and CeO_2(220) measured by in-plane XRD for (a) Si and (b) CeO_2/Si. Ellipses indicate FWHM of diffraction peaks for Si and CeO_2. Incident X-ray angle (α) was 0.2°.

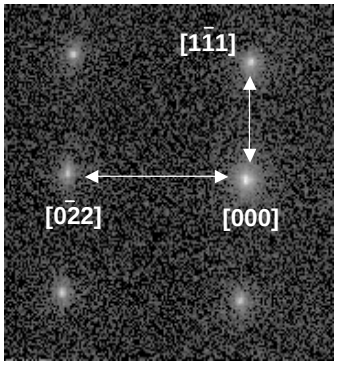

Fig. 4 Electron diffraction pattern (EPD) of CeO_2. Spot positions of CeO_2 [0$\bar{2}$2] and [1$\bar{1}$1] from [000] were compared with those of Si.

Table I Relative changes in CeO_2 (110) and (111) lattice spacings from Si ($\Delta d_{CeO2(110)}$ and $\Delta d_{CeO2(111)}$).

Experimental method	in-plne XRD (±0.02%)	EDP (±0.1%)
$\Delta d_{CeO2(110)}$	+0.26	+0.3
$\Delta d_{CeO2(111)}$	-	+0.3

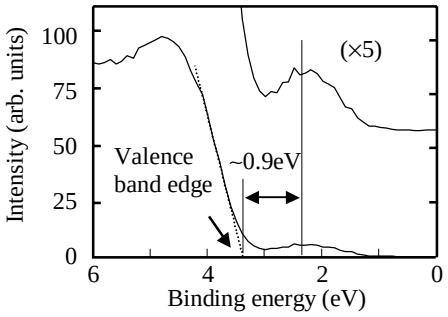

Fig. 5 XPS spectrum of CeO_2 valence band edge. In-gap state (~0.9 eV from the valence band edge) attributed to oxygen defects was observed.

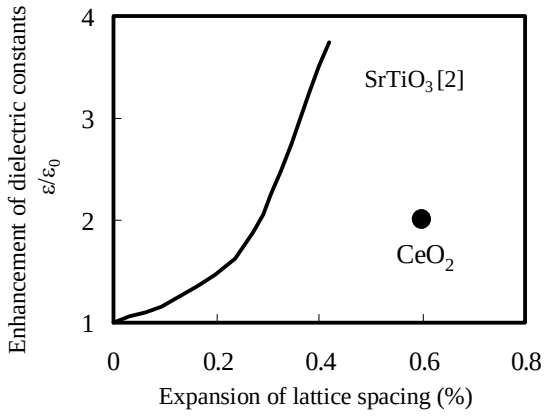

Fig. 6 Relationship between expansion of CeO_2 (111) lattice spacing and enhancement of dielectric constant for CeO_2 compared with $SrTiO_3$ [2] .